

# Mapping the Enzymatic Active Site of *Pseudomonas aeruginosa* Exotoxin A

Barbara J. Brandhuber,<sup>1</sup> Viloya S. Allured,<sup>1</sup> Tanya G. Falbel,<sup>2</sup> and David B. McKay<sup>1</sup>

<sup>1</sup>Departments of Chemistry and Biochemistry and <sup>2</sup>Molecular, Cellular, and Developmental Biology, University of Colorado, Boulder, Colorado 80309

**ABSTRACT** *Pseudomonas aeruginosa* exotoxin A is a representative of a class of enzymes, the mono-ADP-ribosyl transferases, which catalyze the covalent transfer of an ADP-ribose moiety of NAD<sup>+</sup> to a target substrate. Availability of the three-dimensional structure of exotoxin A provides the opportunity for mapping substrate binding sites and suggesting which amino acid residues may be involved in catalysis. Data from several sources have been combined to develop a proposal for the NAD<sup>+</sup> binding site of exotoxin A: the binding of NAD<sup>+</sup> fragments adenosine, AMP, and ADP have been delineated crystallographically to 6.0, 6.0, and 2.7 Å, respectively; significant sequence homology spanning 60 residues has been found between exotoxin A and diphtheria toxin, which has the identical enzymatic activity; iodination of exotoxin A, under conditions in which only tyrosine 481 is iodinated in the enzymatic domain, abolishes ADP-ribosyl transferase activity.

**Key words:** *Pseudomonas* toxin, x-ray crystallography, ADP-ribosyl transferase, sequence homology

## INTRODUCTION

Exotoxin A of *Pseudomonas aeruginosa* is a secreted bacterial toxin which inhibits protein synthesis in target eukaryotic cells by ADP-ribosylation of a specific modified histidine residue (called diphthamide) of protein synthesis elongation factor 2 (EF-2), as the last step of an intoxication process that requires the transmembrane translocation of, at a minimum, the enzymatic domain of the molecule into the target cell cytoplasm.<sup>1</sup> The transfer of a single ADP-ribose moiety from NAD<sup>+</sup> to a target protein is a covalent modification catalyzed by several bacterial toxins and endogenous eukaryotic proteins. Well-characterized representatives of this class of proteins include diphtheria toxin<sup>2</sup> and an endogenous protein of baby hamster kidney cells,<sup>3</sup> which also ADP-ribosylate the diphthamide residue of EF-2; cholera toxin<sup>4</sup> and *Escherichia coli* heat-labile toxin,<sup>5</sup> which ADP-ribosylate the G<sub>s</sub> regulatory protein of adenylate cyclase; and an exotoxin from *Bordetella pertussis*, which ADP-ribosylates the G<sub>i</sub> regulatory subunit.<sup>6</sup> The prevalence of mono(ADP-ribosyl) transferases among

eukaryotic proteins and exotoxins of pathogenic bacteria has generated an interest in determining the mechanism(s) by which they catalyze their reactions.

The three-dimensional structure of an enzyme, taken in conjunction with data from other sources, provides a useful foundation for elucidating its catalytic mechanism. Historically, many inferences regarding enzymatic mechanism have been drawn from the results of chemical modification experiments and substrate or inhibitor binding experiments. Currently, these inferences can be tested explicitly by site-specific mutagenesis.

The three-dimensional structure of one representative of the mono-ADP-ribosyl transferase proteins, exotoxin A of *P. aeruginosa*, has been reported.<sup>7</sup> The molecule has three distinct structural domains (designated I, II, and III); the carboxy-terminal domain III has been identified as the enzymatic domain. The structure solved crystallographically is of the proenzyme form of the molecule, as it is secreted from bacteria, before it enters a target cell and is enzymatically activated; suggestions of enzymatic mechanisms referencing the structure should be interpreted with this caveat.

In this paper we report results from several methods—chemical modification; locating bound fragments of NAD<sup>+</sup> by crystallographic difference Fouriers; homology searches between exotoxin A and diphtheria toxin—which suggest how the substrate NAD<sup>+</sup> may bind to exotoxin A, and which residues may be involved in specific interactions with NAD<sup>+</sup>.

## MATERIALS AND METHODS

### Materials

Purified exotoxin A protein was provided by Dr. John Collier, Harvard Medical School, or purchased from the Swiss Serum and Vaccine Institute, Berne, Switzerland. Exotoxin A crystals were grown as reported.<sup>8</sup> [adenine-2,8-<sup>3</sup>H]-NAD<sup>+</sup> was purchased from

Abbreviations used: DTT, dithiothreitol; TCA, trichloroacetic acid; PEG, polyethylene glycol (average molecular weight 8,000).

Received October 20, 1987; revision accepted January 27, 1988.

Address reprint requests to David B. McKay, Department of Chemistry and Biochemistry, University of Colorado, Campus Box 215, Boulder, CO 80309-0215.

New England Nuclear, Boston, Massachusetts. Other chemicals were purchased from Sigma Chemical, Saint Louis, Missouri.

#### Assay for Enzymatic Activity

Exotoxin A was activated by incubation in 4 M urea, 1 mM DTT (hereafter referred to as "urea plus DTT") for 15 minutes at room temperature. Enzymatic activity was measured by the incorporation of radioactivity from  $^3\text{H-NAD}^+$  into TCA-precipitable material, using crude wheat germ EF-2 as a substrate.<sup>9</sup> Typically, 6  $\mu\text{g}$  of activated exotoxin A was incubated in 200  $\mu\text{l}$  of solution for 30 minutes. When this assay was employed to determine kinetic parameters the exotoxin A concentration was held between 10 nM and 25 nM, while the concentration of  $\text{NAD}^+$  was varied from 0.3  $\mu\text{M}$  to 10  $\mu\text{M}$ .

#### Iodination of Exotoxin A

An " $\text{I}_3^-$  stock" solution, approximately 20 mM  $\text{I}_3^-$  in 20% methanol, was prepared using published procedures,<sup>10</sup> and stored in the dark until use. (Concentrations of  $\text{I}_3^-$  quoted throughout the paper refer to initial concentrations of the reagent used for reactions, made by diluting the  $\text{I}_3^-$  stock solution, and hence assuming 20 mM  $\text{I}_3^-$  concentration before dilution. For crystals, with reaction times 10–100 hours, some evaporation of  $\text{I}_2$  from solution occurred, even in tightly sealed containers; hence concentrations quoted refer to initial values.) To iodinate exotoxin A crystals, the  $\text{I}_3^-$  stock solution was diluted either 1:10 or 1:100 with a crystal stabilization solution, either i) 20% PEG, 1.5 M NaCl, 50 mM potassium phosphate, pH 7.2, or ii) 20% PEG, 1.5 M NaCl, 25 mM sodium citrate, 25 mM sodium acetate, pH 5.5; crystals were allowed to react at room temperature in the dark for times ranging from 4 to 70 hours. Crystals were then back-soaked in the same stabilization solution without the  $\text{I}_3^-$  reagent, prior to data collection or enzymatic assays. To iodinate exotoxin A in solution, the  $\text{I}_3^-$  stock was diluted 1:10 into a solution of 0.9 mg/ml exotoxin A in i) 50 mM Tris HCl, pH 8, or ii) 25 mM sodium citrate, 25 mM sodium acetate, pH 5.5, and allowed to react in the dark at room temperature for a variable length of time. The toxin was then separated from iodination reagent by gel filtration through Sephadex G-50 in the same buffer used in the reaction.

#### Nitration of Exotoxin A

Exotoxin A, 1 mg/ml in 50 mM Tris HCl, pH 8.0, was allowed to react for variable lengths of time with  $5 \times 10^{-4}$  M tetranitromethane (TNM) at room temperature. The reaction was stopped by cooling the reaction vessel in an ice bath; excess reagents were removed by dialysis against the 50 mM Tris HCl buffer.

#### X-Ray Data Collection

Datasets to 6.0 Å resolution were collected by diffractometer; intensity profiles of Bijvoet pairs of re-

flections were recorded using omega step scans across reflection peaks. Background corrections were applied, reflection intensities were integrated, and transmission and radiation decay corrections were computed and applied as previously described.<sup>7</sup> In crystals that had been iodinated, disordering of the crystals and rapid radiation decay precluded data collection to higher resolution. In crystals with other ligands, excessive radiation decay was not a significant problem.

For datasets to 2.7 Å resolution, area detector data were collected on a Xentronics multiwire area detector employing a fine focus ( $0.4 \times 8.0 \text{ mm}^2$ ) stationary target x-ray source operating at 1.2 kW power. An oscillation range of  $0.1^\circ$  per frame and a counting time of  $\sim 300$  seconds per frame were used. Intensities were integrated from oscillation frames using standard programs.<sup>11</sup> Radiation decay parameters were estimated by re-measuring the first  $1^\circ$  of data two or three times during data collection, and fitting a decay correction function of the form:

$$I(t) = I(t=0) [p_1 + p_2 * (1 + p_3 \frac{\sin^2\theta}{\lambda^2}) * t]$$

where  $p_1$ ,  $p_2$ , and  $p_3$  are adjustable parameters, to the integrated intensities; the decay correction is linear in time, with a slope (rate of falloff) which varies with resolution.

#### Computations and Model Building

For 6.0 Å resolution datasets, difference Fouriers between ligand-bound and native crystal data were computed using multiple isomorphous replacement (MIR) phases with an overall figure-of-merit of 0.91.<sup>7</sup> For 2.7 Å resolution datasets, difference Fouriers were computed using MIR phases below 6.0 Å resolution and phase-combined phases above 6.0 Å resolution from the crystallographic refinement of exotoxin A currently in progress. Model building was effected with the molecular modelling program FRODO<sup>12</sup> (version 6.1 from Rice University).

The largest positive peak in the difference Fouriers of iodinated crystals was near one of the heavy atom sites found in two of the derivatives used in phasing; to eliminate the possibility the peak was a heavy atom "ghost," phases were computed with three derivatives which did not have heavy atoms at this site. The subsequent iodine difference Fourier computed with these phases again showed the strongest iodine peak, albeit with a lower signal to background ratio, confirming that the site was real.

#### Sequence Homology Searches

Searches for sequence homology between exotoxin A and diphtheria toxin were effected by computing the number of identical or equivalent amino acids within a sliding window ranging in size from 21 to 51 amino acids in length. Since the arginine to lysine ratio is much higher in the enzymatic domain of

exotoxin A (19 to 3 in residues 401–613) than in the diphtheria toxin fragment A (7 to 16 in residues 1–193), arginine and lysine were considered equivalent, although the results of the searches were not substantially affected by this assumption. No other residues were equivalenced.

## RESULTS

### Iodination and Nitration of Exotoxin A

Datasets collected on crystals soaked in  $I_3^-$  at pH 5.5 for 50–100 hours showed positive difference Fourier peaks; the observed peaks are summarized in Table I. A crystal soaked for 4 hours under the same conditions displayed no difference peaks.

Three sites of iodination were observed in the crystals. The sites were reproducible, with variable relative peak height, for crystals soaked 50 and 100 hours. (Dataset III, a partial dataset with ~50% of the reflections to 6.0 Å resolution, serves to confirm site A in a third, independent dataset. Radiation decay of the crystal precluded collecting a complete 6.0 Å dataset.) Site "A," the strongest peak, was consistently observed near tyrosine 481; the difference peak appears as a single, essentially spherical peak to one side of the phenolic ring (Fig. 1a). The tyrosine appears to be monoiodinated on the  $C_\epsilon$  position, which is readily accessible in the cleft region of domain III of the molecule. Distances between the (unrefined) position of the iodine and the  $C_\epsilon$  position of tyrosine 481 suggest some movement of the side chain probably occurs upon iodination. The iodine- $C_\epsilon$  distance observed in diiodotyrosine in model compound studies is 2.0 Å; errors in the difference map peak positions and the coordinates of the partially refined exotoxin A model probably amount to no more than 1.0 Å; the computed distances to  $C_\epsilon$  of tyrosine 481 for peak A are in the range 3.4–3.6 Å. Minor shifts in tyrosine side chain positions upon iodination are not unanticipated, having previously been observed in crystals of myoglobin<sup>13</sup> and subtilisin BPN'.<sup>14</sup>

A second, weaker site of iodination, peak "B," is near the side chain of tyrosine 289. In contrast to the difference peak at tyrosine 481, peak B is elongated and asymmetric. Its appearance in contour maps strongly suggests a mixture of mono- and diiodotyrosine at residue 289. This result is also not unanticipated; a mixture of mono- and diiodotyrosine as products at a specific residue, with the ratio of the two dependent on reaction time and conditions, has previously been observed and quantified in crystals of chymotrypsin.<sup>10</sup> The distance between iodines in diiodotyrosine is 6.0 Å<sup>15</sup>; data to 6.0 Å resolution would not resolve the two iodines into two discrete peaks. The distances in Table I are the distance between the highest local peak of the difference map and the  $C_\epsilon$  of tyrosine, and in a case where the diiodotyrosine adduct is present, do not strictly represent a  $C_\epsilon$ -iodine distance. The position of the (asymmetric) peak B unambiguously establishes tyrosine 289 as a site of iodination.

In addition to reacting with the phenolic ring of tyrosine, iodination reagents may also react with the imidazole ring of histidines.<sup>16</sup> Peak "C," the third significant iodine site, appears as an essentially spherical peak approximately 2 Å from  $C_\epsilon$  of histidine 118.

Enzymatic activity was measured on protein from redissolved crystals iodinated at pH 5.5, and compared to the activity of protein from native crystals stabilized at the same pH. The amount of protein in a crystal was computed from the volume, estimated from the external dimensions of the crystal. Protein from crystals soaked in 0.2 mM  $I_3^-$  typically retained greater than 70% of its original activity, even after a 70-hour soak. Protein from crystals soaked in 2 mM  $I_3^-$  retained approximately 50% of its original activity after 16 hours; after 70 hours, the activity was reduced to less than 10% of the value expected for native protein. Further, after x-ray data collection, one of the crystals yielding positive difference peaks

TABLE I. Positive Peaks Observed in Difference Fourier Maps for Crystals Soaked in 2 mM  $I_3^-$ , pH 5.5

Dataset	Soak time (hr)	$R_{\text{sym}}^*$	Peak	S/N <sup>†</sup>	Position
I	100	0.042	A	1.9	3.4 Å from $C_\epsilon$ of Tyr 481
			B	1.4	0.9 Å from $C_\epsilon$ of Tyr 289
			C	1.2	2.5 Å from $C_\epsilon$ of His 118
II	50	0.053	A	1.4	3.6 Å from $C_\epsilon$ of Tyr 481
			B	1.3	2.9 Å from $C_\epsilon$ of Tyr 289
			C	1.2	1.6 Å from $C_\epsilon$ of His 118
III‡	50	0.046	A	1.3	3.6 Å from $C_\epsilon$ of Tyr 481

\* $R_{\text{sym}} = \Sigma |I_i - \langle I \rangle| / \Sigma \langle I \rangle$ , where  $I_i$  is  $i$ -th measurement of intensity of a reflection;  $\langle I \rangle$  is its calculated mean value; and the sum is taken over all measured reflections.

†S/N = signal-to-noise, defined as ratio of positive peak height to magnitude of largest negative peak in map.

‡Dataset III is a partial dataset, with ~50% of the reflections to 6.0 Å resolution.

was redissolved and assayed for activity; the protein showed less than 10% of its native activity.

It was consistently observed, therefore, that conditions of iodination that yielded observable crystallographic difference Fourier peaks at specific sites correlated with the loss of most, typically > 90%, of the enzymatic activity of the protein in the crystals. Conditions of iodination which abolished less than 50% of the activity at pH 5.5 did not yield observable difference peaks; presumably in these cases, the extent of iodination, and consequently the occupancy of the iodine sites was too low to yield peaks above the background level of the difference maps.

The low pH, and the apparent iodination at only a small number of major sites, appeared to be a necessary condition for giving interpretable peaks in difference Fouriers. It is expected that the rate of iodination would be significantly more rapid at the higher pH<sup>16</sup>. The rate of loss of enzymatic activity of crystals in 2 mM I<sub>3</sub><sup>-</sup> at pH 7.2 was dramatically higher; protein from redissolved crystals showed no detectable activity after 1 hour of reaction. Six datasets were collected on crystals iodinated at pH 7.2 with 2 mM I<sub>3</sub><sup>-</sup>, for times ranging from 4 hours to 100 hours; none of these datasets showed positive difference peaks. It is probable that the greater extent of iodination anticipated at the higher pH results in an unacceptable loss of isomorphism of the crystals, which in turn would preclude the possibility of observing iodine peaks in the difference Fouriers.

NAD<sup>+</sup> did not appear significantly to protect exotoxin A from loss of activity by iodination. Exotoxin A was reacted with 2 mM I<sub>3</sub><sup>-</sup> in solution under a variety of conditions: both pH 5.5 and pH 8.0; both prior to activation with urea plus DTT and subsequent to activation; for times ranging from 30 minutes to 14 hours; both in the presence and absence of 1 mM NAD<sup>+</sup>. In no case was it observed that NAD<sup>+</sup> gave a substantial protection against loss of enzymatic activity.

It has been reported by other investigators that tetranitromethane inhibits the enzymatic activity of diphtheria toxin by nitration of tyrosine 60 in the enzymatic domain.<sup>17,18</sup> It was, therefore, of interest to determine whether the same reagent would inhibit exotoxin A. Under the conditions described in Materials and Methods, which are similar to those reported for diphtheria toxin, prior to activation with urea plus DTT, exotoxin A was relatively resistant to loss of enzymatic activity; after 20 hours, the protein still retained 50% of its initial activity. However, after being activated with urea plus DTT, the protein had a half-time for loss of activity of 1–2 minutes, which is the same order-of-magnitude as the half-time for loss of diphtheria toxin activity. 20 mM NAD<sup>+</sup> failed to provide activated exotoxin A with any significant protection against loss of enzymatic activity.

### Ligand Binding

Results of the difference Fouriers on ligands are summarized in Table II. At 6.0 Å resolution, adeno-

sine, AMP and ADP give single overlapping peaks of similar size and shape with progressively lower signal-to-noise ratios. A dataset collected to higher resolution on adenosine, including 92% of the possible reflections to 2.7 Å resolution, displayed the overall shape of the adenosine molecule (Fig. 1b). The adenosine is bound with the purine base in a "pocket" within the cleft of domain III. (It is noteworthy that exotoxin A does not have the classical nucleotide binding domain first observed in the dehydrogenases.) No significant negative peaks appeared above the general continuum of negative background in the difference maps; there is no evidence suggesting a substantial conformational change in the exotoxin A molecule upon adenosine binding. Experiments with NAD<sup>+</sup> failed to give a difference density that could be interpreted as a complete NAD<sup>+</sup> molecule.

The difference Fourier results suggest that exotoxin A, in a proenzyme conformation in the crystal, may not bind NAD<sup>+</sup> specifically without a shift in conformation. The results also suggest that the adenosine binding site observed may be the site at which the adenosine moiety of NAD<sup>+</sup> binds in the enzymatically active toxin. Supporting this suggestion is the observation that adenosine is a competitive inhibitor with respect to NAD<sup>+</sup> in the ADP-ribosylation of EF-II, both for a 26-kilodalton (kD) active fragment of exotoxin A (K<sub>I</sub> = 0.1 mM,<sup>19</sup>) and for the activated toxin (K<sub>I</sub> = 0.1 mM, this work).

### Sequence Homology Searches

Sequence homology searches between diphtheria toxin and exotoxin A showed one stretch of approximately 60 amino acids of significant homology within the enzymatic domains (Figs. 2, 3), with one deletion of three amino acids in exotoxin A relative to diphtheria toxin. The deletion is in a region of the sequence that forms an extended loop on the surface of exotoxin A. Within this region, 24 of 60 residues (40% of the residues) are identical or equivalent (Arg=Lys). This homology can be seen clearly in contour plots of the type shown in Figure 2 when windows of 31, 41, or 51 amino acids are used; however, it is not obvious for windows significantly shorter than 21 or longer than 61 amino acids. For small (<21 residues) windows, random homologies give rise to a much higher noise level in the contour maps. Since the homology is

TABLE II. Difference Fourier Results of Ligands Bound to Exotoxin A

Soaking condition	Maximum resolution (Å)	R <sub>sym</sub>	S/N
8 mM adenosine	6.0	0.021	3.3
8 mM adenosine	2.7	0.060	2.6
5 mM AMP	6.0	0.032	1.9
40 mM ADP	6.0	0.046	1.2

Crystals were soaked for 2 days in mother liquor plus the specified ligand. R<sub>sym</sub> and S/N are as defined in Table I.

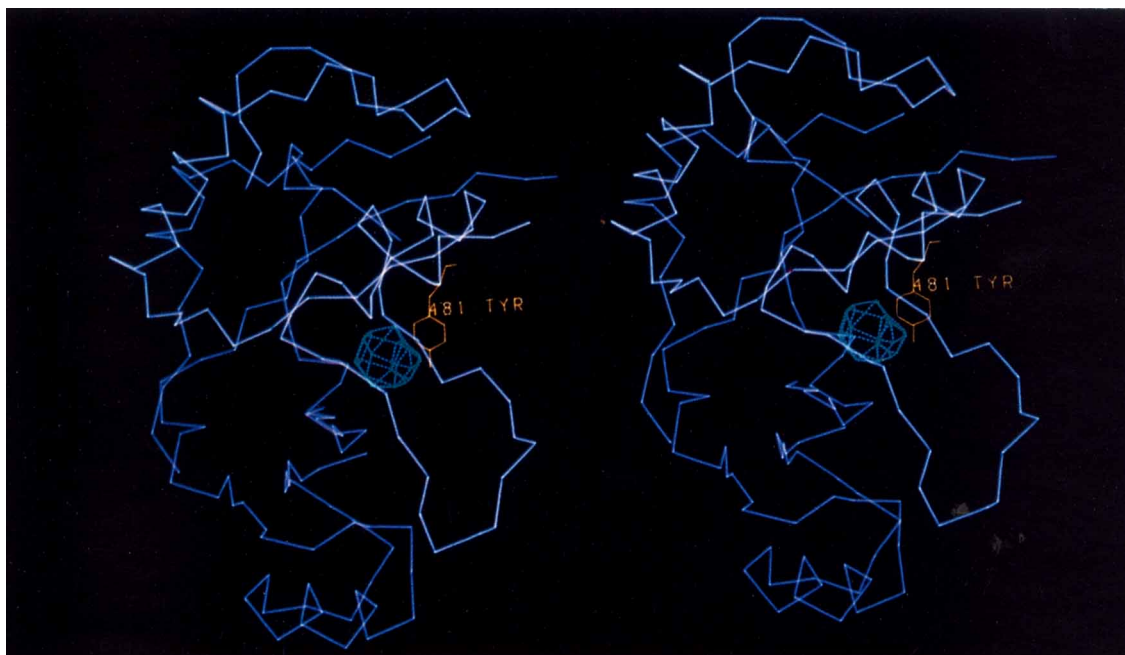


Fig. 1. **a:** Alpha carbon stereo drawing of domain III of exotoxin A (residues 400–613), showing tyrosine 481 and the iodine-native difference Fourier peak, contoured four standard deviation units above the mean value of the difference Fourier map density. Breaks in alpha carbon backbone are as described in reference 7. **b:** Stereo drawing of exotoxin A domain III showing a 2.7 Å resolution adenosine-native difference map contoured four standard deviation units above the mean value of the difference Fourier map density, with an adenosine molecule built into the density. **c:** Stereo drawing of domain III of exotoxin A illustrating a possible binding mode for NAD<sup>+</sup> (shown in green) and the residues homologous with diphtheria toxin (shown in red). Residues proposed to have specific interactions with NAD<sup>+</sup> are labeled.

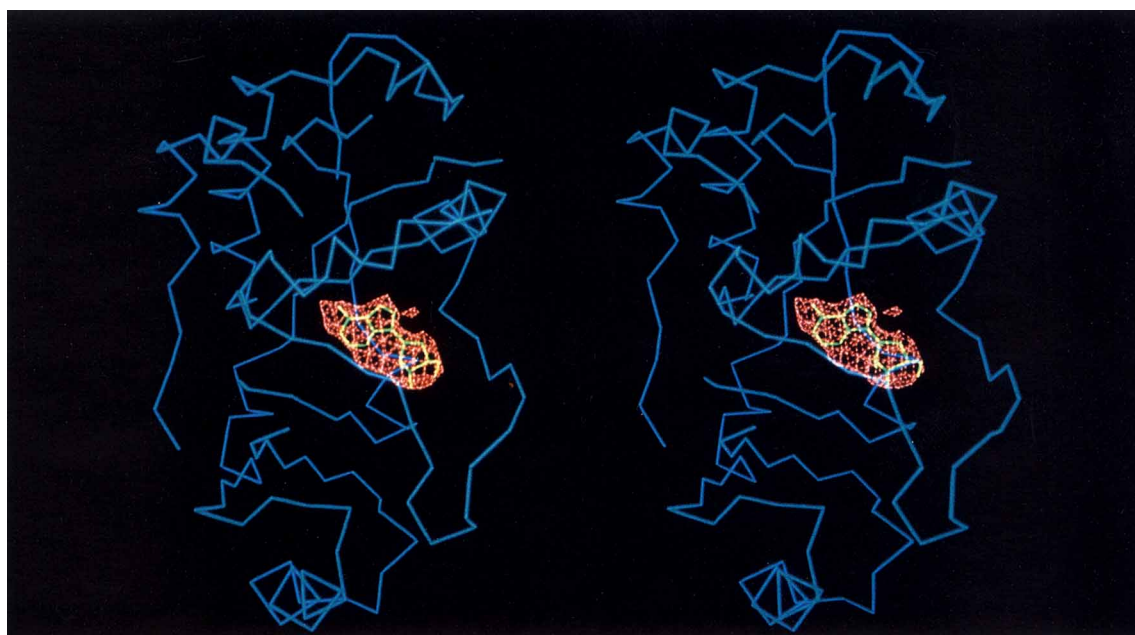


Figure 1b

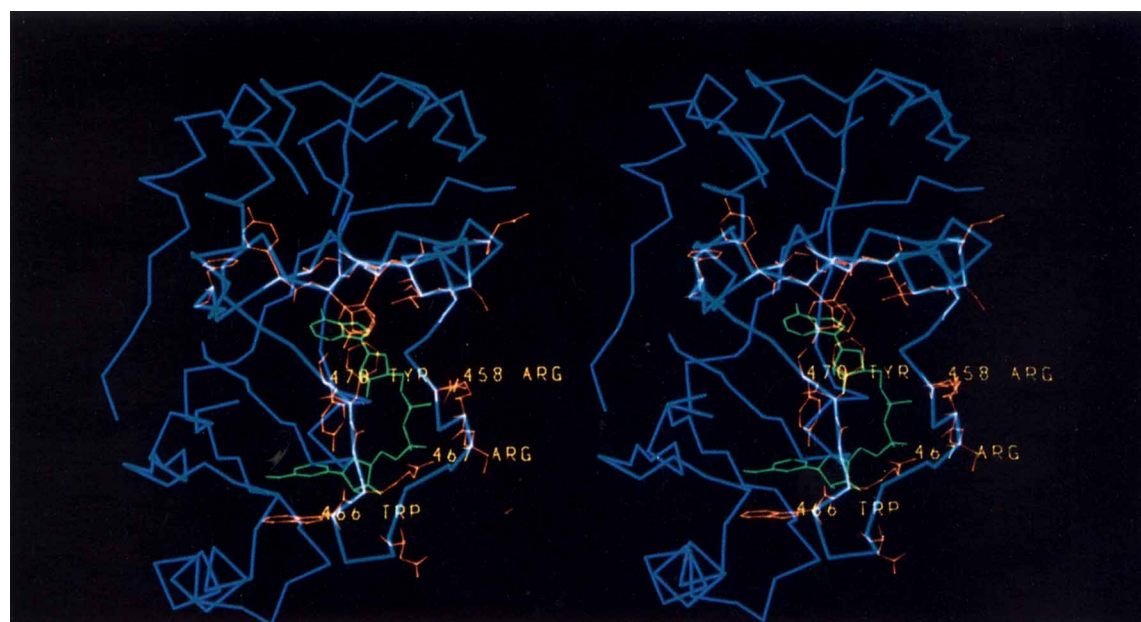


Figure 1c

significant over only a 60-residue segment, for large (>60 residues) windows the signal will be attenuated by non-homologous regions at the ends of the window.

### DISCUSSION

Mapping substrate binding sites by locating bound substrates, substrate fragments, or inhibitors with crystallographic difference Fouriers is a well-established methodology. Particularly relevant in this context is the work of Rossmann and coworkers on binding of coenzyme fragments to lactate dehydrogenase (LDH).<sup>20</sup> Comparisons of the binding of adenosine, AMP, ADP, and NAD<sup>+</sup>, when bound in a binary complex with LDH, and comparisons of their binding in the binary complex to the binding of NAD<sup>+</sup> in a ternary NAD<sup>+</sup>-pyruvate complex, revealed that i) the isolated fragments adenosine, AMP, and ADP bind as isolated molecules in generally the same position and conformation as their moieties on NAD<sup>+</sup>, although ii) there are small but significant shifts, maximally ~2 Å, between atomic positions of bound adenosine, AMP, and ADP, and NAD<sup>+</sup> in the binary complex, as well as iii) shifts of similar magnitude between NAD<sup>+</sup> in the binary and the ternary complexes. This precedent, in combination with the observation that adenosine is a competitive inhibitor of exotoxin A activity, legitimize the assumption that the observed adenosine binding site represents, approximately, the site of binding of the adenosine moiety of NAD<sup>+</sup> on exotoxin A.

Reactions which iodinate tyrosines, and to a lesser extent histidines, are established methods of protein modification.<sup>16</sup> Iodination of tyrosines in protein crystals, and crystallographic determination of their positions, have been reported for myoglobin,<sup>13</sup> papain,<sup>21</sup> and subtilisin BPN'.<sup>14</sup> A thorough study by Sigler of

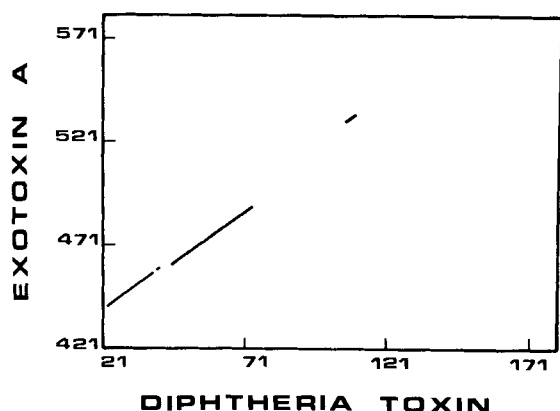


Fig. 2. Contour plot of sequence homology search between exotoxin A and diphtheria toxin. Window size: 41 amino acids; numbers on axes are sequence numbers of center amino acid in window. Contours are plotted 4 sigma (4 times 1.8 amino acids) above the mean (3.3 amino acids) homology for the 41 residue window.

DT	GLY	ALA	ASP	ASP	VAL	VAL	ASP	SER	SER	LYS	10
ETA	GLU	ARG	LEU	LEU	GLN	ALA	HIS	ARG	GLN	LEU	429
DT	SER	PHE	VAL	MET	GLU	ASN	PHE	SER	SER	TYR	20
ETA	GLU	GLU	ARG	GLY	TYR	VAL	PHE	VAL	GLY	TYR	439
DT	HIS	GLY	THR	LYS	PRO	GLY	TYR	VAL	ASP	SER	30
ETA	HIS	GLY	THR	PHE	LEU	GLU	ALA	ALA	GLN	SER	449
DT	ILE	GLN	LYS	GLY	ILE	GLN	LYS	PRO	LYS	SER	40
ETA	ILE	VAL	PHE	GLY	GLY	VAL	ARG	ALA	ARG	SER	459
DT	GLY	THR	GLN	GLY	ASN	TYR	ASP	ASP	ASP	TRP	50
ETA	.....	(GLN	ASP	LEU)	.....	ASP	ALA	ILE	TRP	466	
DT	LYS	GLY	PHE	TYR	SER	THR	ASP	ASN	LYS	TYR	60
ETA	ARG	GLY	PHE	TYR	ILE	ALA	GLY	ASP	PRO	ALA	476
DT	ASP	ALA	ALA	GLY	TYR	SER	VAL	ASP	ASN	GLU	70
ETA	LEU	ALA	TYR	GLY	TYR	ALA	GLN	ASP	GLN	GLU	486
DT	ASN	PRO	LEU	SER	GLY	LYS	76				
ETA	PRO	ASP	ALA	ARG	GLY	ARG	492				

Fig. 3. Sequence alignment showing homology between exotoxin A (ETA) and diphtheria toxin (DT).

iodination of tyrosine 171 in chymotrypsin crystals, with analytical quantitation of the mono- and diiodo-tyrosine products and a demonstration of correlation between iodinated products observed analytically and iodine peaks observed in crystallographic difference Fouriers, established the reliability of interpreting crystallographic difference Fourier peaks as iodines covalently bound to amino acid residues.<sup>10</sup>

Of the three iodine sites observed, only site A near tyrosine 481 lies within domain III, the carboxy terminal domain, of exotoxin A. Site B, near tyrosine 289, is within domain II, the helical domain; site C near histidine 118 is within the antiparallel beta sheet of domain I. The side chain of tyrosine 481 extends into the cleft region of domain III that was previously suggested, based on the three-dimensional structure of the molecule, to be the enzymatic domain.<sup>7</sup> In a strict interpretation, the alternative possibility that iodination at the sites outside domain III interfere with enzymatic activation under denaturing conditions cannot be excluded, although the fact that iodination under similar conditions after enzymatic activation also abolishes activity argues against this possibility. Iodination of tyrosine 481 therefore appears to be responsible for the loss of enzymatic activity of exotoxin A. Loss of activity by itself does not distinguish between the alternative possibilities that i) tyrosine 481 is an essential catalytic residue which participates directly in the ADP-ribosyl transferase reaction, ii) tyrosine 481 is not essential for catalysis,



but modification of it blocks productive substrate binding, or iii) the loss of activity is due to oxidation of another residue such as histidine by the iodination reagent, which would not be visible in the difference Fourier, and the iodination of tyrosine 481 is coincidental. The model proposed below for  $\text{NAD}^+$  binding supports the second of these alternatives.

The enzymatic moieties of diphtheria toxin and exotoxin A catalyze the identical ADP-ribosyl transferase reaction, with similar catalytic constants;<sup>9</sup> it is probable that the two enzymes utilize identical or similar catalytic residues, and have structurally similar substrate binding pockets. Supporting this suggestion is the fact that both proteins, when activated, can be photolabeled by  $\text{NAD}^+$ , with the concomitant loss of enzymatic activity, at a specific glutamic acid residue (Glu 148 in diphtheria toxin;<sup>22</sup> Glu 553 in exotoxin A<sup>23</sup>). However, when the nucleotide sequences, and by implication, the amino acid sequences, for the two proteins were determined and compared, no homology was reported.<sup>24-26</sup> The results presented here demonstrate homology within a limited region of the enzymatic domains which, by normal criteria, is somewhat weak. However, examination of the identical or equivalent residues in the three-dimensional model of exotoxin A reveals almost all of them to lie in the active site cleft of the molecule (Fig. 1c). The limited sequence homology apparently represents a strong similarity in substrate recognition site, manifesting the shared necessity of the two molecules to bind and act catalytically upon identical substrates.

We have modeled possible modes of interaction of  $\text{NAD}^+$  with exotoxin A by superimposing its adenosine moiety on the adenosine position determined crystallographically and adjusting the remainder of the molecule. The modeling exercise suggests a binding mode for  $\text{NAD}^+$  (Fig. 1c) which requires only minor shifts ( $< 1 \text{ \AA}$ ) in the backbone and side chain positions of the exotoxin A model. It is apparent that in this proposed binding site, most of the interactions of  $\text{NAD}^+$  with exotoxin A would be with residues that are homologous in diphtheria toxin; the two molecules would have nearly identical  $\text{NAD}^+$  binding sites.

The ligand binding, chemical modification, and sequence homology results do not provide definitive proof of the  $\text{NAD}^+$  binding model shown in Figure 1c: rather, they present a set of self-consistent data that yield a model that can be readily tested by site-specific mutagenesis. In particular, the nicotinamide ring of  $\text{NAD}^+$  would stack on the indole ring of Trp 466 (Trp 50 in diphtheria toxin), and could be responsible for the tryptophan fluorescence quenching reported for diphtheria toxin<sup>27</sup> and an exotoxin A enzymatically active fragment.<sup>9</sup> The positively charged side chains of Arg 458 and Arg 467 (Lys 39 and Lys 51 in diphtheria toxin) could form ionic salt bridges with the negatively charged phosphates of

$\text{NAD}^+$ . Replacement of these residues with uncharged residues, such as methionines, should substantially reduce the affinity of the molecules for  $\text{NAD}^+$ . The phenolic hydroxyl of Tyr 470 (Tyr 54 in diphtheria toxin) would be positioned near the nicotinamide-ribose bond broken during catalysis; whether Tyr 470 participates directly in catalysis could be tested by examining whether replacing it with phenylalanine abolishes activity. The phenolic ring of Tyr 481 (Tyr 65 in diphtheria toxin) appears to interact with the purine ring of the adenosine moiety, but is remote from the proposed catalytic site. It is apparent in this model that abolition of enzymatic activity by iodination of Tyr 481 could result from steric hindrance of  $\text{NAD}^+$  or other substrate binding; if this were the case, replacement of this tyrosine with phenylalanine should not dramatically affect enzymatic activity. Experiments testing these suggestions are currently in progress (R.J. Collier, personal communication).

## ACKNOWLEDGMENTS

This work was supported by award AI-19762 and Research Career Development Award AI-00631 from the National Institutes of Health (NIH) to D.B.M., postdoctoral fellowship PF-2317 from the American Cancer Society to V.S.A., a predoctoral stipend from NIH training grant GM-07135 to T.G.F., and awards AI-22021 and CA-39217 from NIH to R. John Collier.

## REFERENCES

1. Iglewski, B.H., Kabat, D.  $\text{NAD}$ -dependent inhibition of protein synthesis by *Pseudomonas aeruginosa* toxin. *Proc. Natl. Acad. Sci. U.S.A.* 72:2284-2288, 1975.
2. Collier, R.J. Effect of diphtheria toxin on protein synthesis: Inactivation of one of the transfer factors. *J. Mol. Biol.* 25:83-89, 1967.
3. Lee, H., Iglewski, W.J. Cellular ADP-ribosyltransferase with the same mechanism of action as diphtheria toxin and *Pseudomonas* toxin A. *Proc. Natl. Acad. Sci. U.S.A.* 81:2703-2707, 1984.
4. Moss, J., Richardson, S. Activation of adenylate cyclase by heat-labile *Escherichia coli* enterotoxin. *J. Clin. Invest.* 62:281-285, 1982.
5. Gill, D.M. Involvement of nicotinamide adenine dinucleotide in the action of cholera toxin *in vitro*. *Proc. Natl. Acad. Sci. U.S.A.* 72:2064-2068, 1975.
6. Katada, T., Ue, M. ADP ribosylation of the specific membrane protein of C6 cells by islet-activating protein associated with modification of adenylate cyclase activity. *J. Biol. Chem.* 257:7210-7216, 1982.
7. Allured, V.A., Collier, R.J., Carroll, S.F., McKay, D.B. Structure of exotoxin A of *Pseudomonas aeruginosa* at 3.0 Angstrom resolution. *Proc. Natl. Acad. Sci. U.S.A.* 83:1320-1324, 1986.
8. Collier, R.J., McKay, D.B. Crystallization of exotoxin A from *Pseudomonas aeruginosa*. *J. Mol. Biol.* 157:413-415, 1982.
9. Chung, D.W., Collier, R.J. Enzymatically active peptide from the adenosine diphosphate-ribosylating toxin of *Pseudomonas aeruginosa*. *Infect. Immun.* 16:832-841, 1977.
10. Sigler, P.B. Iodination of a single tyrosine in crystals of  $\alpha$ -chymotrypsin. *Biochemistry* 18:3609-3617, 1979.
11. Durbin, R.M., Burns, R., Moulai, J., Metcalf, P., Freymann, D., Blum, M., Anderson, J.E., Harrison, S.C., Wiley, D.C. Protein, DNA, and virus crystallography with a focused imaging proportional counter. *Science* 232:1127-1132, 1986.
12. Jones, T.A. A graphics model building and refinement system for macromolecules. *J. Appl. Crystallogr.* 11:268-272, 1978.



13. Kretsinger, R.H. A crystallographic study of iodinated sperm whale metmyoglobin. *J. Mol. Biol.* 31:315-318, 1968.
14. Wright, C.S., Alden, R.A., Kraut, J. Structure of subtilisin BPN' at 2.5 Å resolution. *Nature* 221:235-242, 1969.
15. Hamilton, J.A., Steinrauf, L.K. Crystallographic studies of iodine-containing amino acids. *Acta Cryst.* A23:817-825, 1967.
16. Roholt, O.A., Pressman, D. Iodination-isolation of peptides from the active sites. *Methods Enzymol.* 25:438-449, 1972.
17. Beugnier, N., Zanen, J. Diphtheria toxin: The effect of nitration and reductive methylation on enzymatic activity and toxicity. *Biochim. Biophys. Acta* 490:225-234, 1977.
18. Delaunoy, J.P., Zanen, J. Diphtheria toxin: Implication of tyrosine 60 in the adenosine binding site for the substrate NAD. *Toxicon* 20:257-258, 1982.
19. Lory, S., Collier, R.J. Expression of enzymic activity by exotoxin A from *Pseudomonas aeruginosa*. *Infect. Immun.* 28:494-501, 1980.
20. Chandrasekhar, K., McPherson, A., Adams, M.J., Rossmann, M.G. Conformation of coenzyme fragments when bound to lactate dehydrogenase. *J. Mol. Biol.* 76:503-518, 1973.
21. Drenth, J., Jansonius, J.N., Koekoek, R., Swen, H.M., Wolthers, B.G. Structure of Papain. *Nature* 218:929-932, 1968.
22. Carroll, S.F., McCloskey, J.A., Crain, P.F., Oppenheimer, N.J., Marschner, T. M., Collier, R.J. Photoaffinity labeling of diphtheria toxin fragment A with NAD: structure of the photoproduct at position 148. *Proc. Natl. Acad. Sci. U.S.A.* 82:7237-7241, 1985.
23. Carroll, S.F., Collier, R.J. Active site of *Pseudomonas aeruginosa* exotoxin A. Glutamic acid 553 is photolabeled by NAD and shows functional homology with glutamic acid 148 of diphtheria toxin. *J. Biol. Chem.* 262:8707-8711, 1987.
24. Gray, G.L., Smith, D.H., Baldrige, J.S., Harkins, R.N., Vasil, M.L., Chen, E.Y., Heyneker, H.L. Cloning, nucleotide sequence, and expression in *Escherichia coli* of the exotoxin A structural gene of *Pseudomonas aeruginosa*. *Proc. Natl. Acad. Sci. U.S.A.* 81:2645-2649, 1984.
25. Greenfield, L., Bjorn, M.J., Horn, G., Fong, D., Buck, G.A., Collier, R.J., Kaplan, D.A. Nucleotide sequence of the structural gene for diphtheria toxin carried by corynebacteriophage  $\beta$ . *Proc. Natl. Acad. Sci. U.S.A.* 80:6853-6857, 1983.
26. Ratti, G., Rappouli, R., Giannini, G. The complete nucleotide sequence of the gene coding for diphtheria toxin in the corynebacteriophage  $\omega$  (tox<sup>+</sup>) genome. *Nucl. Acids Res.* 11:6589-6595, 1983.
27. Kandel, J., Collier, R.J., Chung, D.W. Interaction of fragment A from diphtheria toxin with nicotinamide adenine dinucleotide. *J. Biol. Chem.* 249:2088-2097, 1974.